

Article

Implementation of a Four-Class Motor Imagery Brain Computer Interface Using Long Short-Term Memory Neural Network

Hao-Teng Hsu *, Kuo-Kai Shyu and Po-Lei Lee

Department of Electrical Engineering, National Central University, No. 300, Zhongda Rd., Jongli District, Taoyuan City 32001, Taiwan;

kkshyu@ee.ncu.edu.tw (K.-K. Shyu); pllee@ee.ncu.edu.tw (P.-L. Lee)

* Correspondence: fifaworld91@g.ncu.edu.tw; Tel.: +886921722775

Received: Feb 4, 2022; Accepted: Mar 4, 2022; Published: Mar 30, 2022

Abstract: We have developed multi-channel dry-electrode electroencephalography (EEG) system to implement a brain computer interface (BCI) and discriminate four-class motor imagery signals. The EEG channels recorded from Fz, F3, F4, C3, Cz, C4, P3, and P4 positions, according to the international 10–20 EEG system, were acquired and wirelessly transmitted to a personal computer. Five subjects were recruited to perform right hand, left hand, right foot, and left foot imagery movements with 60 trials in each movement type. EEG data were segmented into epochs from 0 to 8 s and anchored to time points of imagery movement cues. The segmented EEG epochs were pre-processed using the Morlet wavelet. A long short-term memory (LSTM) neural network with 64 LSTM cells was constructed to discriminate EEG signals recorded from different imagery movements. Among total EEG epochs, 80% were randomly chosen as training data and the rest 20% were used as validation data. The detection accuracy reached 89%.

Keywords: Brain computer interface (BCI), Long short-term memory (LSTM) neural network, Motor imagery movement

1. Introduction

Stroke p Paralyzed patients who are incapable of moving their limbs voluntarily due to patients, brain injury patients, or amyotrophic lateral sclerosis (ALS) are unable to communicate with external environments. A technique such as a brain computer interface (BCI) enables users to help paralyzed patients express their intentions and communicate via their brain waves. However, due to the large inter-individual variations of brain waves, the most challenging issue in designing a BCI system is how to define an effective classifier for discerning brain wave patterns induced from distinct tasks. Several signal processing techniques or classifiers have been developed to achieve a high-performance BCI system. Xu et al. developed an enhanced probabilistic linear discriminant analysis (LDA) method to achieve multi-class classification BCI in motor imagery tasks [1]. Yazdani et al. applied k-nearest neighbor (KNN) to discriminate different mental tasks [2]. Hsu et al. adopted an adaptive neuron-fuzzy classifier to classify four options in a phase-tagged steady-state visual evoked potential (SSVEP) based BCI system [3]. Kumar et al. used particle swarm optimization (PSO) for feature selection in a motor imagery BCI system [4]. Nevertheless, most motor imagery BCIs with classifiers differentiate only two imagery movements. Only few research groups succeeded in classifying four or more mental tasks. Accordingly, in this study, we adopted a deep learning technique to classify four motor imagery tasks by applying a long short-term memory (LSTM) neural network.

2. Materials and Methods

Five healthy subjects, four males and one female, aged 25.2 ± 3.3 years old, were recruited for this study. All participants submitted informed consent to the institutional review board (IRB), Taoyuan General Hospital, Taiwan (TYGH107055). An eight-channel wireless EEG system (InMex EEG, WellFulfill Co., Taiwan), certificated by IEC 60601-1-2 for electricity safety was used to record motor-related EEG signals. The EEG signals were recorded at 1000 Hz with a 24-bits resolution. Each EEG dry electrode was constructed by 10 spring-loaded copper pins, and its biocompatibility has been certificated by ISO 10993. The EEG channels of Fz, F3, F4, C3, Cz, C4, P3, and P4 positions were acquired and wirelessly transmitted to a personal computer according to the international 10-20 EEG system. The eight-channel dry-electrode EEG system is shown in Fig. 1.

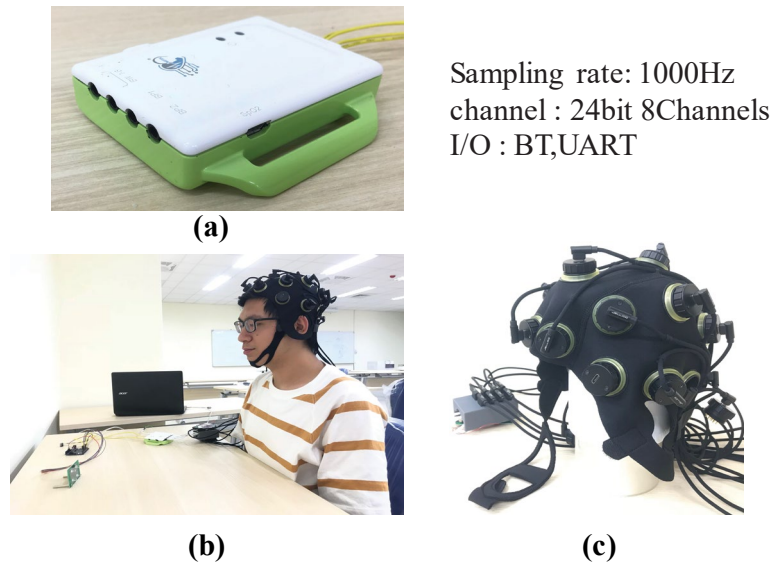


Fig. 1. Photographs of the eight-channel dry-electrode EEG system. (a) EEG amplifier (b) Measurement environment (c) Dry-electrode EEG cap.

Fig. 2 illustrates the experimental diagram of this study. Subjects were requested to sit comfortably in an armchair. A 32-inch LCD monitor was placed 50 cm in front of the subjects. Each epoch was designed to last nine-second long. After the presence of a visual cue with a beep sound, the subjects were requested to perform a designated motor imagery task, preceded by a three-second silent counting. In this study, the type of motor imagery task in each trial was indicated by the visual cue, which was one of the four imagery movements, including right hand, left hand, right foot, and left foot movements.

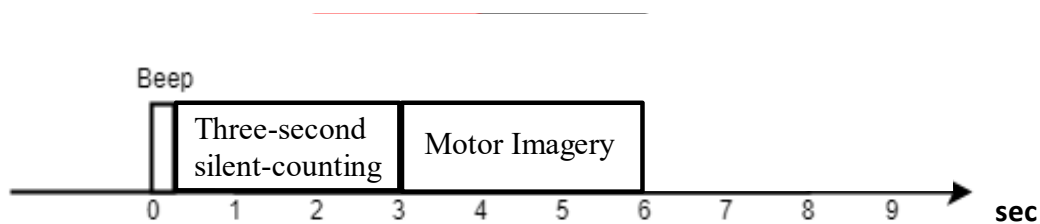


Fig. 2. Experimental paradigm of our motor imagery movements.

The acquired EEG data were segmented in each epoch from 0 to 8 s and anchored to the visual cue (or beep sound), which covered around one second preceding the onset of motor imagery movement and the whole period of motor imagery movement. The four-second EEG epochs were preprocessed using the Morlet wavelet to obtain temporal-frequency features. The obtained temporal-frequency features were used as input data to train the LSTM neural network. Since EEG features usually have large fluctuations, the EEG signals were averaged every two seconds, in which the data during 0–8 s were averaged to produce four values, presenting the average values for 0–2, 2–4, 4–6, and 6–8 s. Considering the frequency information of 1–37 Hz, the input vector of each trial for LSTM was 37 (frequency) \times 8 (channel) \times 4 (time information) which provided 1184 features. The signal preprocess is presented in Fig. 3.

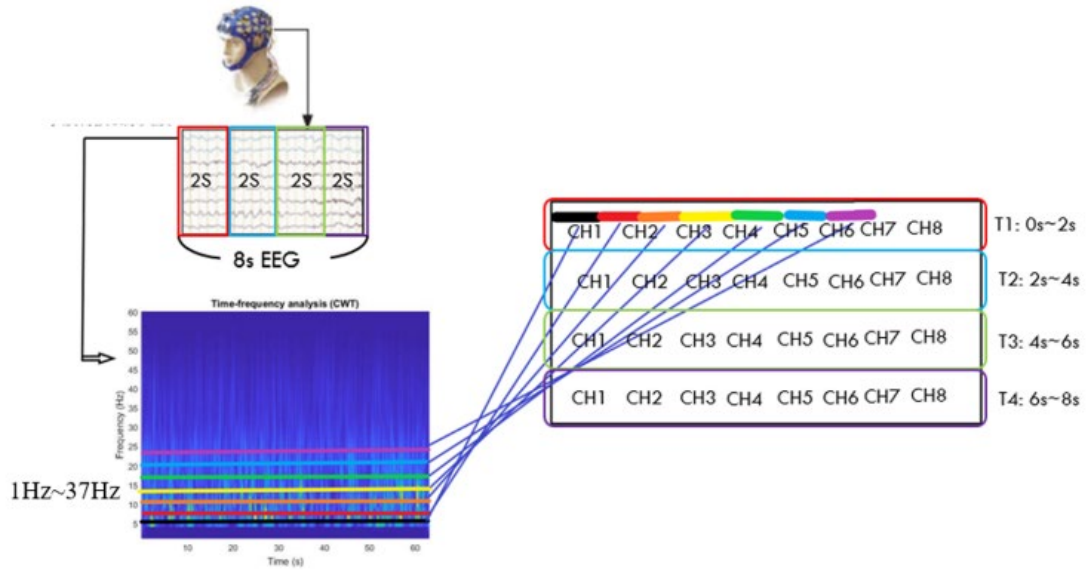


Fig. 3. Signal preprocessing of EEG temporal-frequency features.

The LSTM model in this study had 64 LSTM cells and 48 hidden neurons. The signal processing was written in python language on Keras 3.0 platform with TensorFlow 2.0 as the backend. The LSTM model is shown in Fig. 4.

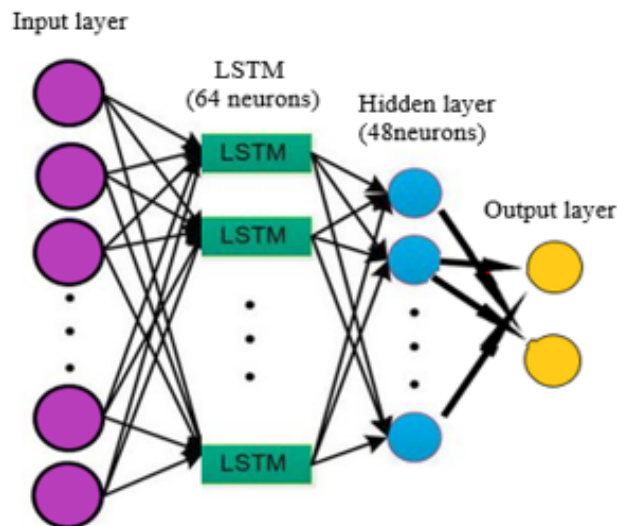


Fig. 4. LSTM model in this study.

3. Results

Figs. 5 and 6 show the temporal-frequency features on C3 and C4 of the motor imagery movements of subjects S1 and S2, respectively. Different patterns among these four imagery movements were observed in the movements. The obtained temporal-frequency features were rearranged into the input vector with 1184 features of the LSTM neural network model. Fig. 7 presents the training and testing accuracies versus the training epoch number in this study. The training accuracy reached higher than 95% after more than 125 training epochs. However, the testing accuracy was 89% after applying more than 175 training epochs.

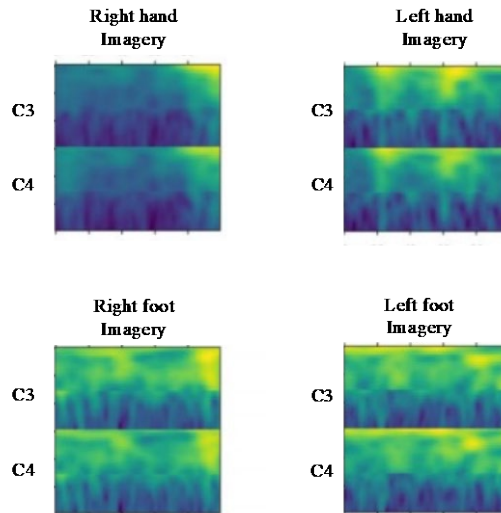


Fig. 5. Temporal-frequency features on C3 and C4 of the motor imagery movements in subject S1.

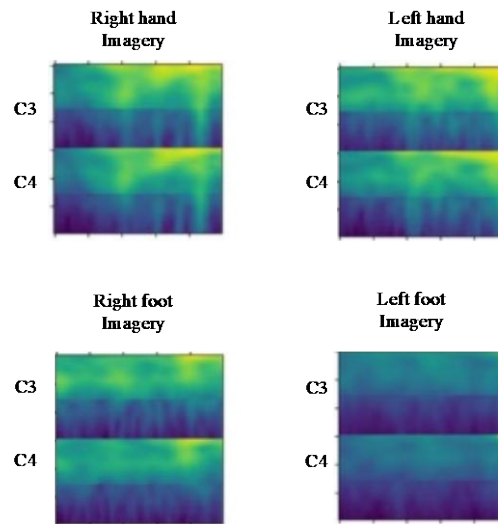


Fig. 6. Temporal-frequency features on C3 and C4 of the motor imagery movements in subject S2.

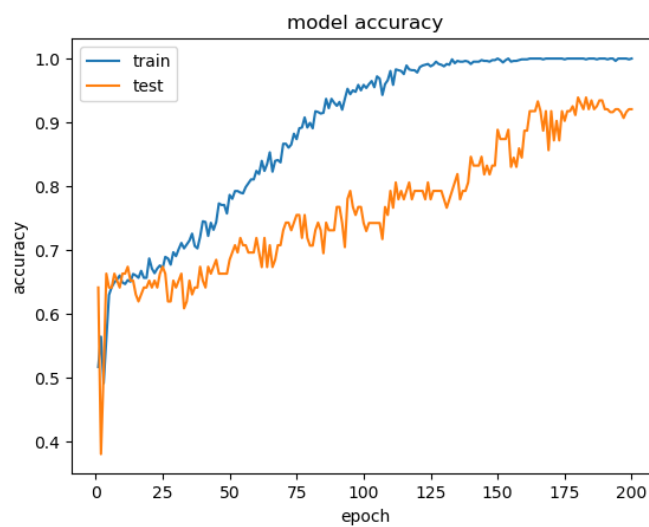


Fig. 7. Training and testing results of the LSTM neural network in motor imagery BCI tasks.

In order to obtain the optimal time segments, we compared the four different time segments, including -2-6, 0-8, 2-10, and 4-12 s. The mean accuracies were 61.81, 89.61, 88.29, and 85.44 % in each time segment. The highest accuracy is 89.61 % in 0-8 s, which means that the specific pattern appeared in 8 s from the onset of the motor imagery. The accuracies for the five subjects are shown in Table 1.

Table 1. Accuracy of the input vector for the LSTM model in different time segments.

| Subject | Accuracy (%) | | | |
|---------|----------------|---------|----------|----------|
| | Times Segments | | | |
| | -2~6 sec | 0~8 sec | 2~10 sec | 4~12 sec |
| SubA | 62.14 | 86.77 | 89.13 | 85 |
| SubB | 58.45 | 84.31 | 85.46 | 81.78 |
| SubC | 60.12 | 87.64 | 87.77 | 84.51 |
| SubD | 66.45 | 95.71 | 91.65 | 89.61 |
| SubE | 61.88 | 93.61 | 87.46 | 86.32 |
| mean | 61.81 | 89.61 | 88.29 | 85.44 |

The accuracies of traditional SVM and the radial basis function (RBF) SVM were 52 and 67%, and the detection accuracy for CNN was 77%. The lower accuracies of SVM were caused by the fact that the causal relationship was embedded in the acquired EEG data. Though the utilization of the temporal-frequency features of the whole EEG epoch as a feature map for CNN also includes the causal information of motor imagery movement, the 2D CNN needs to be considered with the topology arrangement of EEG features from different channels to optimize the 2D arrangement. The results of SVMs, CNN, and LSTM are shown in Table 2.

Table 2. The detection results of SVM, CNN, and LSTM.

| | SVM Model | | Deep Learning | |
|----------|------------|---------|---------------|------|
| | SVM-Linear | SVM-rbf | CNN | LSTM |
| Accuracy | 0.52 | 0.67 | 0.77 | 0.89 |

4. Conclusions

In this study, we have demonstrated the effectiveness of LSTM for classifying EEG data in a four-class motor imagery task. To validate the effectiveness, the results from the traditional SVM, RBF-SVM, and CNN were compared with that of LSTM. The study results showed the LSTM achieved better detection than the other three classifiers. In contrast to previous motor imagery studies in which only two motor imagery movements were classified, a high classification rate was achieved in discriminating four mental patterns, which is the main contribution of this study. In the future, it is necessary to design biofeedback and enhance the stimulation feedback of the efferent-to-afferent neural loop. Other neural networks, such as reinforcement learning networks, will be adopted in future studies.

Author Contributions: Contributions are listed as follows: conceptualization, P.-L. Lee and K.-K. Shyu; methodology, H.-T. Hsu; software, H.-T. Hsu; validation, H.-T. Hsu; formal analysis, H.-T. Hsu; investigation, P.-L. Lee; writing—original draft preparation, H.-T. Hsu and P.-L. Lee; writing—review and editing, H.-T. Hsu and P.-L. Lee; visualization, K.-K. Shyu.

Funding: This study was funded by the National Central University, Ministry of Science and Technology (MOST 111-2217-E-008-001-MY3, 110-2923-E-008-002-MY3, 110-2221-E-008-095-MY3, 110-2634-F-008-007, 110-2634-F-A49-004, 107-2912-I-008-511), Taoyuan General Hospital Intramural Project.

Conflicts of Interest: The authors declare no conflict of interest.

References

- Xu, P.; Yang, P.; Lei, X.; Yao, D. An enhanced probabilistic LDA for multi-class brain computer interface. *PLoS One* **2011**, *6*(1): e14634.
- Yazdani, A.; Ebrahimi, T.; Hoffmann, U. Classification of EEG signals using Dempster Shafer theory and a k-nearest neighbor classifier. In Proceedings of the 4th International IEEE/EMBS Conference on Neural Engineering, 2009, pp. 327-330.
- Hsu, H.-T.; Lee, P.-L.; Shyu, K.-K. Improvement of classification accuracy in a phase-tagged steady-state visual evoked potential-based brain-computer Interface using adaptive neuron-fuzzy classifier. *International Journal of Fuzzy Systems* **2017**, *19*(2), 542-552.

4. Kumar, S.U.; Inbarani, H.H. PSO-based feature selection and neighborhood rough set-based classification for BCI multiclass motor imagery task. *Neural Computing and Applications* **2017**, *28*(11), 3239–3258.

Publisher's Note: IJKII stays neutral with regard to jurisdictional claims in published maps and institutional affiliations.

Copyright: © 2022 The Author(s). Published with license by IJKII, Singapore. This is an Open Access article distributed under the terms of the [Creative Commons Attribution License](https://creativecommons.org/licenses/by/4.0/) (CC BY), which permits unrestricted use, distribution, and reproduction in any medium, provided the original author and source are credited.